Journal of Visualized Experiments

A murine model of ischemic retinal injury induced by transient bilateral common carotid artery occlusion

--Manuscript Draft--

Article Type:	Invited Methods Article - JoVE Produced Video
Manuscript Number:	JoVE61865R2
Full Title:	A murine model of ischemic retinal injury induced by transient bilateral common carotid artery occlusion
Corresponding Author:	Toshihide Kurihara Keio University School of Medicine Shinjuku-ku, Tokyo JAPAN
Corresponding Author's Institution:	Keio University School of Medicine
Corresponding Author E-Mail:	kurihara@z8.keio.jp
Order of Authors:	Deokho Lee
	Yukihiro Miwa
	Heonuk Jeong
	Shin-ichi Ikeda
	Yusaku Katada
	Kazuo Tsubota
	Toshihide Kurihara
Additional Information:	
Question	**Response**
Please indicate whether this article will be Standard Access or Open Access.	Standard Access (US$2,400)
Please indicate the **city, state/province, and country** where this article will be **filmed**. Please do not use abbreviations.	Shinjuku-ku, Tokyo, Japan
Please confirm that you have read and agree to the terms and conditions of the author license agreement that applies below:	I agree to the Author License Agreement
Please specify the section of the submitted manuscript.	Medicine
Please provide any comments to the journal here.	

TITLE:

A murine model of ischemic retinal injury induced by transient bilateral common carotid artery occlusion

AUTHORS AND AFFILIATIONS:

Deokho Lee[1,2,*], Yukihiro Miwa[1,2,3,*], Heonuk Jeong[1,2], Shin-ichi Ikeda[1,2], Yusaku Katada[1,2], Kazuo Tsubota[1,2,4] and Toshihide Kurihara[1,2]

[1]Laboratory of Photobiology, Keio University School of Medicine, Tokyo, Japan
[2]Department of Ophthalmology, Keio University School of Medicine, Tokyo, Japan
[3]Animal eye care, Tokyo Animal Eye Clinic, Tokyo, Japan
[4]Tsubota Laboratory, Inc., Tokyo, Japan

[*]These authors contributed equally to this work.

Corresponding authors
Toshihide Kurihara
E-mail: kurihara@z8.keio.jp

Kazuo Tsubota
E-mail: tsubota@z3.keio.jp

Co-authors
Deokho Lee: deokholee@keio.jp
Yukihiro Miwa: yukihiro226@gmail.com
Heonuk Jeong: jeong.h@keio.jp
Shin-ichi Ikeda: muscle.s.ikeda@gmail.com
Yusaku Katada: yusakukatada@z2.keio.jp

KEYWORDS:

Carotid artery occlusion; Electroretinography; Experimental models; Hypoxia; Ischemia; Optical coherence tomography; Retina; Reperfusion

SUMMARY:

Here, we describe a mouse model of retinal ischemia by transient bilateral common carotid artery occlusion using simple sutures and a clamp. This model can be useful for understanding the pathological mechanisms of retinal ischemia caused by cardiovascular abnormalities.

ABSTRACT:

Diverse vascular diseases such as diabetic retinopathy, occlusion of retinal veins or arteries and ocular ischemic syndrome can lead to retinal ischemia. To investigate pathological mechanisms of retinal ischemia, relevant experimental models need to be developed. Anatomically, a main retinal blood supplying vessel is the ophthalmic artery (OpA) and OpA originates from the internal carotid artery of the common carotid artery (CCA). Thus, disruption of CCA could

effectively cause retinal ischemia. Here, we established a mouse model of retinal ischemia by transient bilateral common carotid artery occlusion (tBCCAO) to tie the right CCA with 6-0 silk sutures and to occlude the left CCA transiently for 2 seconds via a clamp, and showed that tBCCAO could induce acute retinal ischemia leading to retinal dysfunction. The current method reduces reliance on surgical instruments by only using surgical needles and a clamp, shortens occlusion time to minimize unexpected animal death, which is often seen in mouse models of middle cerebral artery occlusion, and maintains reproducibility of common retinal ischemic findings. The model can be utilized to investigate the pathophysiology of ischemic retinopathies in mice and further can be used for in vivo drug screening.

INTRODUCTION:

The retina is a neurosensory tissue for visual function. Since a substantial amount of oxygen is needed for visual function, the retina is known as one of the highest oxygen demanding tissues in the body[1]. The retina is susceptible to vascular diseases as oxygen is delivered through blood vessels. Various types of vascular diseases, such as diabetic retinopathy and retinal blood vessel (veins or arteries) occlusion, can induce retinal ischemia. To investigate pathological mechanisms of retinal ischemia, reproducible and clinically relevant experimental models of retinal ischemia are considered necessary. Middle cerebral artery occlusion (MCAO) by insertion of an intraluminal filament is the most generally utilized method for the development of in vivo rodent models of experimental cerebral ischemia[2,3]. Due to the proximity of the ophthalmic artery (OpA) to MCA, MCAO models are also used simultaneously to understand the pathophysiology of retinal ischemia[4-6]. To induce cerebral ischemia along with retinal ischemia, long filaments are typically inserted through incision of the common carotid artery (CCA) or the external carotid artery (ECA). These methods are difficult to perform, require a long time to complete the surgery (over 60 minutes for one mouse), and lead to high variabilities in the outcomes after the surgery[7]. It remains important to develop a better model to improve these concerns.

In this study, we simply used short transient bilateral CCA occlusion (tBCCAO) with needles and a clamp to induce retinal ischemia in mice and analyzed typical results of ischemic injuries in the retina. In this video, we will give a demonstration of the tBCCAO procedure.

PROTOCOL:

All methods described here have been approved by the Institutional Animal Care and Use Committee (IACUC) of Keio University School of Medicine.

1. Preparation of surgical instruments and animals

1.1. Autoclave surgical instruments and keep them in 70% ethyl alcohol. Prior to each new surgical procedure, clean surgical instruments carefully using 70% ethyl alcohol.

1.2. Prepare male BALB/cAJc1 mice (6 weeks old, 26-28 kg) in a specific-pathogen-free (SPF) room to maintain sterile conditions before, during and after the surgery.

2. Transient bilateral common carotid artery occlusion (tBCCAO)

2.1. Put a mouse under anesthesia via intraperitoneal injection with a combination of midazolam (40 µg/100 µL), medetomidine (7.5 µg/100 µL) and butorphanol tartrate (50 µg/100 µL), termed "MMB", as previously described[8,9]. Hold the mouse's back skins to keep the mouse away from bumping its eyes until the mouse is completely anesthetized.

2.1.1. Judge the depth of anesthesia by pinching the mouse toe until it has no response, of which method is commonly used for checking complete anesthesia[10].

NOTE: Generally, less than 5 min are required for mice to fall asleep. Proper recipes for general anesthesia may be different by institutions.

2.2. Apply one drop of 0.1% purified sodium hyaluronate eye drop solution to the eyes to prevent dryness on the eyes under anesthesia.

2.3. Place the mouse on its back and fix the mouse's paws using adhesive tapes.

2.4. Disinfect the neck area of the mouse using 70% ethyl alcohol before the surgery.

NOTE: Additional clipping of the fur was not performed as this may cause subsequent skin inflammation[11,12].

2.5. Perform sagittal incision of the neck by a scissor (**Figure 1**).

NOTE: Incision needs to be made on the midline between the neck, sternum and trachea.

2.6. Separate both salivary glands carefully using two forceps and mobilize them to visualize the underlying CCAs.

2.7. Isolate the right CCA carefully from the respective vagal nerves and accompanying veins without harming their structures, and place two 6-0 silk sutures under the CCA. Tie the two ties tightly to block the blood flow (**Figure 1**).

NOTE: During the procedure, small veins could be damaged. If bleeding is seen, wiping is required to visualize the CCAs clearly.

2.8. Find the left CCA carefully from the respective vagal nerves and accompanying veins without harming their structures, and occlude the left CCA for 2 seconds by a clamp (**Figure 1**).

NOTE: A 6-0 silk suture needle is needed to be placed under the left CCA to mark a site for clamping.

2.9. After reopening of the left CCA, suture wounds of the neck by a 6-0 silk suture and apply a dab of antibiotic (50 µL) onto the neck to inhibit bacterial infection.

NOTE: Softly remove a clamp to avoid damaging the arterial wall when reopening of the left CCA.

2.10. Inject 0.75 mg/kg of atipamezole hydrochloride intraperitoneally to the mice to help the mouse recovered from deep anesthesia quickly. Return the mouse to a mouse cage with pre-heated pads.

NOTE: Do not let the mouse left unattended until the mouse regains sufficient consciousness to maintain sternal recumbency.

2.11. Inject 0.4 mg/kg of butorphanol tartrate to the mouse for the management of pain when the mouse wakes up.

NOTE: The protocol can be paused here. As a first hint for successful tBCCAO, eyelid drooping of the mouse can be observed (**Figure 2**).

2.12. For euthanasia, inject 3x of MMB mixture to the mice and sacrifice them for experiments.

3. General observations (survival rates and eyelid drooping)

3.1. After the surgery, check survival rates for all causes of death at day 0 (after the surgery), 1, 3 and 7.

3.2. Assess eyelid drooping by a 4-point rating scale: 1 = no drooping, 2 = mild drooping (~50%), 3 = severe drooping (over 50%), and 4 = severe drooping with eye discharge.

4. Retinal blood perfusion

4.1. Inject 200 µL of FITC-dextran (25 mg/mL) into the left ventricle of the mouse, which is commonly used for the observation of blood perfusion in mouse retinal vessels[13,14].

4.2. 2 minutes after circulation, enucleate the eyes and fix in 4% paraformaldehyde for 1 hour. The retinas were carefully obtained and flat-mounted, as previously described[15], and examined via a fluorescence microscope.

4.3. Take photographs of the retinal whole mounts at 4x magnification and merge into a single using a merge analyzer, previously described[16].

4.4. Measure the perfused areas via a vessel analysis tool in NIH Fiji/ImageJ software.

5. Western blot

5.1. 3 and 6 hours after tBCCAO, obtain the eyes of mice and immediately transfer to a Petri dish containing cold PBS to isolate the retinas.

5.2. After isolation of the retinas, perform western blotting, as previously described[9].

5.3. Incubate with antibodies for hypoxia-inducible factor-1α (HIF-1α; a general hypoxia marker) and for β-Actin (an internal loading control) overnight followed by incubation of HRP-conjugated secondary antibodies. Visualize the signals via chemiluminescence.

6. Quantitative PCR (qPCR)

6.1. 6, 12 and 24 hours after tBCCAO, process the obtained retinas for qPCR, as previously described[17].

6.2. Perform qPCR via real-time PCR system. Primers used are listed in **Table 1**. Calculate fold changes between levels of different transcripts by the $\Delta\Delta C_T$ method.

7. Immunohistochemistry (IHC)

7.1. 3 days after tBCCAO, obtain the eyes of mice and embed in paraffin.

7.2. Cut the paraffin-embedded eyes by a microtome to obtain the eye sections.

7.3. De-paraffinize and stain the eye sections of 5 μm thickness as previously described[13].

7.4. Incubate with an antibody for glial fibrillary acidic protein (GFAP; a reliable marker for astrocytes and Müller cells in the retina) overnight followed by incubation of Alexa Fluor 555-conjugated secondary antibody.

7.5. Use DAPI (4',6-diamidino-2-phenylindole) for staining the nucleus in the retina. Visualize signals via a fluorescence microscope.

7.6. Assess morphology scoring by a 4-point rating scale, as previously described[13,18]: 0 = no signal, 1 = few positive glial end-feet in the ganglion cell layer (GCL), 2 = few labelled processes reaching from GCL to the outer nuclear layer (ONL), and 3 = most labelled processes reaching from GCL to ONL.

8. Electroretinography (ERG)

8.1. 3 and 7 days after tBCCAO, perform ERG using a Ganzfeld dome, acquisition system and LED stimulators, as previously described[9].

8.2. Following dark adaptation overnight, anesthetize mice with a combination of MMB under dim red light.

8.3. Use a mixed solution of 0.5% tropicamide and 0.5% phenylephrine to dilate the pupils.

8.4. Record the active electrodes with contact lens electrodes and place the reference electrode in the mouth.

8.5. Obtain ERG responses from both eyes of each animal.

8.6. Record scotopic responses under dark adaptation with various stimuli.

8.7. Measure the amplitudes of a-wave from the baseline to the lowest point of a-wave.

8.8. Measure the amplitudes of b-wave from the lowest point of a-wave to the peak of b-wave.

8.9. Keep all mice warm during the procedure using heat pads.

9. Optical coherence tomography (OCT)

9.1. 2 weeks after tBCCAO, perform OCT using SD-OCT system, as previously reported[8,9].

9.2. For the measurement, subject mice to mydriasis by a mixed solution of 0.5% tropicamide and 0.5% phenylephrine, and under general anesthesia by a mixture of MMB.

9.3. Obtain B scan images from equatorial slices of en-face scans.

9.4. Examine the retinas at 0.2, 0.4 and 0.6 mm from the optic nerve head.

9.5. Measure retinal thickness from the retinal nerve fiber layer (NFL) to the external limiting membrane (ELM), and t=consider the average of measured values as retinal thickness of an individual mouse.

9.6. Plot the results as spider diagrams.

REPRESENTATIVE RESULTS:

After systemic circulation of FITC-dextran for 2 minutes, retinal vasculatures of the left and right retinas in the sham-operated mice and tBCCAO-operated mice were examined (**Supplementary Figure 1**). FITC-dextran was fully visible in the both retinas in the sham-operated mice and the left retina in the tBCCAO-operated mice, while it was partially detectible in the right retina in the tBCCAO-operated mice.

After tBCCAO, eyelid drooping was examined (**Figure 2**). The right eyes showed mild (score 2;

75%) and severe eyelid (score 3 and 4; 25%) drooping, while the left eyes had no drooping (score 1; 93.75%) except for one mouse (score 2; 6.25%). Although severe eyelid drooping with eye discharge was not considerably observed in the tBCCAO-operated mice, we could see one mouse for this phenotype (score 4; 6.25%).

Reduced oxygen status in tissues leads to stabilization of HIF-1α and induction of a number of hypoxia-responsive genes such as *EPO*, *VEGF* and *BNIP3*[19-21]. First of all, molecular biological hypoxia using a general hypoxic marker HIF-1α was evaluated via western blotting (**Figure 3**). Increased HIF-1α expression was significantly observed in the right retina 3 and 6 hours after tBCCAO. Next, expressions of hypoxia-responsive genes were evaluated via qPCR (**Supplementary Figure 2**). There was no significant change in hypoxia-responsive gene expressions 6 hours after tBCCAO. 12 hours after tBCCAO, we found *Binp3* expression significantly increased and a slight increase in *Epo* expression was shown in the right retina. 24 hours after tBCCAO, we could also find a slight increase in *Epo* expression in the right retina although it was not statistically significant. *Vegf* expression was not altered from 6 to 24 hours in tBCCAO-operated mice.

Retinal reactive gliosis was examined 3 days after tBCCAO (**Figure 4**), as glia such as astrocytes and Müller cells have been closely associated with retinal ischemia[22]. GFAP has been widely used for detection of astrocytes and Müller cells in the retina[23]. The average of morphology scores for GFAP labelling in the right retina was the highest among the both retinas in the sham-operated mice and the left retina in tBCCAO-operated mice. Based on the localization of GFAP expression, a change in morphology in GFAP labelling is considered to reflect activation of Müller cells.

ERG was used to examine retinal dysfunction after tBCCAO (**Figure 5**). The amplitudes of b-wave in the right eye dramatically decreased 3 and 7 days after tBCCAO. However, the amplitudes of a-wave in the right eye were not significantly changed. When it comes to the left eye, we could not see any changes in the amplitudes of a- and b-waves (**Supplementary Figure 3**).

We performed OCT to determine an alteration in retinal thickness after tBCCAO (**Figure 6**). Retinal thickness in the right eye dramatically increased 2 weeks after tBCCAO, while there was no difference in retinal thickness in the left eye between the tBCCAO- and sham-operated mice.

FIGURE AND TABLE LEGENDS:

Figure 1: Schematic of the model procedure and blood circulation in the circle of Willis. A schematic illustration showed the tBCCAO-induced retinal ischemic mouse model procedure and blood circulation to the retina. CCA, ECA, ICA, PCA and OpA represent the common carotid artery, external carotid artery, internal carotid artery, posterior communicating artery and ophthalmic artery, respectively.

Figure 2: Eyelid drooping after tBCCAO. The severity of eyelid drooping was assessed by 4-point rating based on the reference images: 1 = no drooping, 2 = mild drooping (~50%

drooping), 3 = severe drooping (over 50% drooping), and 4 = severe drooping with eye discharge. Eyelid drooping was observed after tBCCAO and it was maintained during the experimental observation. The results (sham: n = 10, tBCCAO: n = 16) were plotted as a scatter dot plot.

Figure 3: HIF-1α stabilization after tBCCAO. Representative immunoblots and quantitative analyses (groups for hour 3; sham: n = 3, tBCCAO: n = 6 and groups for hour 6; sham and tBCCAO: n = 6) for HIF-1α and β-Actin showed that HIF-1α was stabilized in the right retina 3 and 6 hours after tBCCAO. *P < 0.05. The data were analyzed using Student's *t*-test and presented as mean with ±standard deviation. L and R stand for the left and right retina, respectively.

Figure 4: Reactive gliosis after tBCCAO. Representative sagittal sections of the retinas (sham: n = 4, tBCCAO: n = 4) and quantitative analyses of GFAP labelling (red) by a morphology scoring (0–3) showed that GFAP labelling, mostly restricted in NFL+GCL, was expanded to the entire inner layer, from GCL to ONL (white arrows) in the right retina after tBCCAO. Scale bars, 50 µm. DAPI (blue) was used for staining the nucleus in the retina. NFL, GCL, IPL, INL and ONL represent the nerve fiber layer, ganglion cell layer, inner plexiform layer, inner nuclear layer and outer nuclear layer, respectively. The data was analyzed using Student's *t*-test and presented as median with interquartile range, the 25th and 75th percentile. *P < 0.05. L and R stand for the left and right retina, respectively.

Figure 5: Visual dysfunction in the right eye after tBCCAO. (**A**) Representative waveforms of dark-adapted ERG performed 3 and 7 days after tBCCAO. Stimulation intensity (cd.s/m^2): 0.005. (**B**) Quantitative analyses showed that there was a decrease in the amplitudes of b-wave in the right eye (sham: n = 5, tBCCAO: n = 6) while the amplitudes of a-wave were not changed. *P < 0.05, **P < 0.01. The data were analyzed using Student's *t*-test and presented as mean with ±standard deviation.

Figure 6: A change in retinal thickness after tBCCAO. Representative OCT images in the sham- and tBCCAO-operated retinas and quantitative analyses showed that there was an increase in retinal thickness in the right retina (sham: n = 4, tBCCAO: n = 8). There was no change in the retinal thickness in the left retina (sham: n = 4, tBCCAO: n = 8). Scale bars are 200 (upper) and 100 (lower) µm, respectively. *P < 0.05. The values in the horizontal axis of the diagrams represent 0.2, 0.4 and 0.6 mm distant from the optic nerve head (0) which was detected by the green line. The data were analyzed using two-way ANOVA followed by a Bonferroni post hoc test. Spider diagrams were presented as mean with ± standard deviation. NFL, INL, ONL and ELM are the nerve fiber layer, inner nuclear layer, outer nuclear layer and external limiting membrane, respectively.

Supplementary Figure 1: Retinal blood perfusion after tBCCAO. Representative retinal flat mount images (with higher-magnification of each image) after 2 min of FITC-dextran circulation and quantitative analyses showed that full perfusion was observable in the both retinas in the sham-operated mice and the left retina in the tBCCAO-operated mice. However, the right retina

in the tBCCAO-operated mice showed partial blood perfusion. The data were analyzed using Student's *t*-test and presented as mean with ±standard deviation. L and R stand for the left and right retina, respectively. Scale bars are 800 and 400 μm, respectively.

Supplementary Figure 2: Expressions of hypoxia-responsive genes after tBCCAO. Quantitative analyses showed a transient increase in *Bnip3* mRNA expression in the right retina with statistical significance 12 hours after tBCCAO. *Epo* mRNA expression showed an increasing tendency in the right retina for 24 hours after tBCCAO, although its values were not significantly different in comparison with the sham-operated right retina. **P < 0.01. The data were analyzed using Student's *t*-test and presented as mean with ±standard deviation.

Supplementary Figure 3: Visual function in the left eye after tBCCAO. Quantitative analyses showed that there was no change in the amplitudes of a- and b-waves in the left eye (sham: n = 5, tBCCAO: n = 6). P > 0.05. The data were analyzed using Student's *t*-test and presented as mean with ±standard deviation.

Supplementary Figure 4: Survival rates after tBCCAO in C57BL6 and BALB. Kaplan-Meier survival curves demonstrated that almost all mice died within 3 days after tBCCAO in C57BL6 mice. When it comes to BALB mice, longer clamping time in tBCCAO induces sudden and severe animal death (survival rates on day 7, 20 sec: 10%, 10 sec: 20%, 2 sec: 81%, and 0 sec: 95%).

Supplementary Figure 5: HIF-1α stabilization after unilateral CCAO. A representative immunoblot and quantitative analysis (sham: n = 3, unilateral CCAO: n = 3) for HIF-1α and β-Actin showed that HIF-1α was not stabilized in the retinas 3 hours after unilateral CCAO. P > 0.05. The data was analyzed using Student's *t*-test and presented as mean with ±standard deviation. L and R stand for the left and right retina, respectively.

Supplementary Figure 6: Severe eyelid drooping after tBCCAO with long clamping time. 10 seconds of tBCCAO induced severe eyelid drooping, which was assessed by a 4-point rating scale: 1 = no drooping, 2 = mild drooping (~50%), 3 = severe drooping (over 50%), and 4 = severe drooping with eye discharge, as described in Figure 2.

DISCUSSION:

In the study, we have shown that tBCCAO, using simple sutures and a clamp, could induce retinal ischemia and accompanying retinal dysfunction. Furthermore, we have demonstrated our current protocol for the development of a mouse model of retinal ischemia is easier and faster in comparison with other previous protocols for the development of retinal ischemic injury models[2,3,7].

Anatomically, the left and right cerebral arteries can be connected via posterior communicating arteries (PCAs) which provide collateral circulation in the circle of Willis to maintain adequate blood supply to the central nervous system against flow interruption from occlusions or stenosis of individual vessels[24,25] (**Figure 1**). Lee et al. demonstrated retinal blood perfusion could be 10 min-delayed (which is not an entire blockade of retinal blood perfusion in the

ipsilateral retina) by permanent unilateral CCAO in C57BL6 mice[13]. This implies that induction of retinal ischemia by CCAO is closely associated with conditions of collateral circulation in the circle of Willis. C57BL6 is known to be the most susceptible mouse strain to cerebral ischemia by BCCAO among seven mouse strains including our current study's mouse strain BALB[26]. Due to the incomplete circle of Willis in C57BL6, interruption of brain blood supply from both CCAs induces severe damages in the central nervous system, finally leading to death. In addition, in our preliminary study, we failed to induce tBCCAO in C57BL6 as almost all of the mice (about 80%) died within 3 days after the surgery (**Supplementary Figure 4**). Therefore, we applied tBCCAO to another mouse strain BALB for our current study.

To induce acute retinal ischemic injuries in our BALB model, the right CCA was permanently ligated and the left CCA was applied to boost acute retinal ischemic stress through transient occlusion. This is because mice could not tolerate ischemic stress induced by permanent BCCAO unlike rats who have the complete circle of Willis[27]. Next, we attempted to optimize occlusion time: left CCAO (0-20 seconds), as occlusion time has been considered one of key factors that impacts ischemic injuries to the central nervous system and directly connects with survival rates of experimental models[28,29]. We found that survival rates of BALB mice decreased in an occlusion time-dependent manner (**Supplementary Figure 4**). Occlusion of the left CCA over 10 seconds showed severely higher death rates (over 50%), while occlusion of the left CCA for 2 seconds or no occlusion (or unilateral CCAO) showed relatively higher survival rates (over 80%). Therefore, we excluded the groups (of occlusion time which is 10 and 20 seconds) for the further experiments as efficient and cost-effective experiments cannot be available. Next, we examined whether occlusion of the left CCA for 2 seconds or no occlusion (or unilateral CCAO) could induce retinal hypoxia. HIF-1α is a major regulator functioning in hypoxic responses and is stabilized under hypoxic conditions[30]. In this regard, HIF-1α stabilization has been used as a general molecular biological marker for hypoxia. We could not detect HIF-1α stabilization in the retina in the group of unilateral CCAO (**Supplementary Figure 5**). Interestingly, we could detect HIF-1α stabilization in the group of 2 seconds of tBCCAO (**Figure 3**). This implies retinal hypoxic stress could be induced by 2 seconds of tBCCAO in BALB mice. Therefore, 2 seconds of clamping time were finally selected for our study based on high survival rates after the surgery and induction of retinal ischemia via HIF-1α stabilization.

Although the right CCA was permanently occluded in tBCCAO-operated mice, blood perfusion was partially detected in the right retina 2 minutes after systemic circulation of FITC-dextran (**Supplementary Figure 1**). Furthermore, we found that an alteration in HIF-1α stabilization was not detected in the right retina in the unilateral CCAO-operated BALB mice. This phenomenon could be explained by effects of collateral circulation through the circle of Willis to maintain blood supply to the retina (**Figure 1**). Even though we could not clearly understand effects of left transient CCAO on blood perfusion to the right retina, transient left CCAO along with permanent right CCAO may boost acute hypoxic insults in the right retina as evidenced by a significant change in HIF-1α expression in the right retina after tBCCAO (**Figure 3**). In addition, survival rates of mice were dependent on occlusion time of the left CCA. Taken together, the intensity of retinal ischemic stress could be controlled via left CCAO.

The phenotype of a droopy eyelid has been suggested as a presenting sign or a pathophysiological symptom of severe neurological conditions, especially ischemic stroke[31,32]. The muscle associated with a droopy eyelid is levator palpebrae superioris[33]. This muscle is supplied by the lateral palpebral artery which is one of branches derived from OpA. Hence, when OpA, which supplies the retina, is affected, eyelid drooping could be seen. Eyelid drooping was observed in MCAO mouse models[34], which was also reproduced in our tBCCAO model. Moreover, we described that eyelid drooping becomes severe when occlusion time of the left CCA takes longer (**Figure 2** and **Supplementary Figure 6**). This implies that the severity of eyelid drooping (indirectly referred to as the intensity of retinal ischemic stress) could be dependent on occlusion time of left CCA.

Retinal dysfunction is one of results seen in retinal ischemic retinopathies including stenosis of BCCA in mice[35] and BCCAO in rats[36]. We found that the amplitudes of b-wave decreased in the tBCCAO-operated mice. Several previous studies demonstrated that MCAO also caused a reduction in the amplitude of b-wave after the surgery[37,38]. b-wave reflects a physiological condition of cells in the retinal inner layers, including bipolar cells and Müller cells[39]. Furthermore, reactive gliosis by Müller cells was detected in the inner retinal layer after tBCCAO. This result is also reproduced in MCAO models[40,41] and other CCAO models[13,42]. Taken together, it implies that inner retinal dysfunction could be induced by tBCCAO. Retinal thickness has been reported to increase transiently in acute retinal ischemia[43,44]. We also reproduced this finding in the tBCCAO-operated mice. This data shows that the impairment of blood circulation by tBCCAO could reach the retina and finally affect retinal layers.

For consistent outcomes, anesthetic time and length of surgical procedures as well as other factors such as weights and ages of experimental models and their body temperatures during and after the surgery should be standardized[45]. Particularly, attention is needed to maintain body temperature of mice throughout the experimental observation period. This is because hypothermia could have a preconditioning effect and interfere with ischemic effects by tBCCAO[46]. Even though we could not measure exact body temperature of the mice in our experiments, we used heating pads to warm the mice until the mice regained sufficient consciousness. Furthermore, we compared the tBCCAO-operated mice with the sham-operated mice to control potential confounding effects of uncontrollable factors.

Mouse strains could be an additional important variable factor to induce retinal ischemic injury by tBCCAO. Substantial variation of the circle of Willis in mouse strains could result in an unwanted reduction or induction of cerebral ischemia including retinal ishcemia[47] and thereby could lead to variabilities of the results. Adjustment of clamping time is recommended for a successful tBCCAO-induced ischemic retinopathy when other strains of mice are required to be applied.

In general, incidents of stroke or other brain injuries are invariably accompanied with temporary or permanent vison loss[48]. To date, MCAO mouse model is widely used for stroke studies. As OpA originates proximal to the origin of MCA, any hindrance in the blood flow in MCA obstructs the flow to the retina. Retinal ischemia was firstly demonstrated in rats by

MCAO[37]. Later, the same retinal ischemic model was applied to mice[49]. However, for the procedure, occlusion takes more than 60 minutes and finding an occlusion site is extremely difficult as MCA is buried deep inside the brain. Furthermore, the filament size and insertion length for MCAO greatly decides success of the surgery. Those additional variable factors induce variabilities of the ischemic outcomes after the surgery. Although direct comparison studies are needed between tBCCAO and MCAO, we described the beneficial features of our experimental models in this study: short occlusion time, simple experimental procedure and highly accessible occlusion sites. This model may solve the concerns seen in MCAO models.

While the use of the mouse model of retinal ischemia has great benefits for studying retinal ischemic injury, there remain limitations to this approach. Since surgical incision into the neck, separation of the salivary glands and occlusion in the right CCA with sutures must be applied for the procedure, the accompanying tissue disruptions can evoke associated inflammation systemically or at least locally. These concerns were partially addressed using the sham-operated mice, where all the surgical steps are all conducted without tBCCAO. Another issue is a requirement of managing pain that occurs during and after the surgery. In our study, pain management to prevent suffering of the mice was applied through the injection of butorphanol tartrate solution, a synthetically derived opioid agonist-antagonist analgesic of the phenanthrene series. It might be important to be aware that the use of different types of anesthetics and analgesics can disrupt effects of tBCCAO on retinal ischemia. Another limitation to this approach (along with the approaches of currently used other models) is that it does not provide a perfect simulation of pathologies associated with human cardiovascular retinal disorders. To date, mouse models used for such experiments do not suffer from co-morbidities that underlie ischemic retinopathies in humans, mainly with metabolic syndrome such as diabetes[50]. Such complications which are not present in current mouse models could have negative synergistic effects on the pathological pathways for the development of ischemic retinopathies. Therefore, this should be taken into account when interpreting the outcomes from the currently used experimental models including our tBCCAO mouse model. To better understand pathophysiological mechanisms of ischemic retinopathies in humans, our model can be combined with other pathological factors such as streptozotocin injection[51] or high fat diet supplement[52] for the development of ischemic diabetic retinopathy. At last, even though we showed reduced retinal blood perfusion in the tBCCAO-operated mice, we could not clearly understand effects of left transient CCAO on blood perfusion to the right retina. This matter could be addressed using laser-Doppler which is typically used to confirm that occlusion has taken place and ischemia has occurred in vivo in real time[53,54]. This technique could be utilized for better understanding of retinal ischemia in an individual tBCCAO-operated mouse, regarding the collateral circulation in the circle of Willis.

Despite these limitations, our tBCCAO method described here represents an effective approach to produce retinal ischemia in mice. Studying retinal changes by tBCCAO helps to unravel pathological mechanisms of ischemic retinopathies in humans. Furthermore, we hope that tBCCAO mouse model could be used for in vivo drug screening.

ACKNOWLEDGMENTS:

This work was supported by Grants-in-Aid for Scientific Research (KAKENHI) (18K09424 to Toshihide Kurihara and 20K18393 to Yukihiro Miwa) from the Ministry of Education, Culture, Sports, Science and Technology (MEXT).

DISCLOSURES:

The authors have nothing to disclose.

REFERENCES:

1 Anderson, B. Ocular effects of changes in oxygen and carbon dioxide tension. *Transactions of the American Ophthalmological Society.* **66**, 423-474 (1968).

2 Ingberg, E., Dock, H., Theodorsson, E., Theodorsson, A., Ström, J. O. Method parameters' impact on mortality and variability in mouse stroke experiments: a meta-analysis. *Scientific Reports.* **6** (1), 21086 (2016).

3 Atochin Dmitriy, N., Clark, J., Demchenko Ivan, T., Moskowitz Michael, A., Huang Paul, L. Rapid Cerebral Ischemic Preconditioning in Mice Deficient in Endothelial and Neuronal Nitric Oxide Synthases. *Stroke.* **34** (5), 1299-1303 (2003).

4 Allen, R. S. et al. Severity of middle cerebral artery occlusion determines retinal deficits in rats. *Experimental Neurology.* **254**, 206-215 (2014).

5 Steele Ernest, C., Guo, Q., Namura, S. Filamentous Middle Cerebral Artery Occlusion Causes Ischemic Damage to the Retina in Mice. *Stroke.* **39** (7), 2099-2104 (2008).

6 Minhas, G., Morishita, R., Anand, A. Preclinical models to investigate retinal ischemia: advances and drawbacks. *Frontiers in Neurology.* **3**, 75-75 (2012).

7 McColl, B. W., Carswell, H. V., McCulloch, J., Horsburgh, K. Extension of cerebral hypoperfusion and ischaemic pathology beyond MCA territory after intraluminal filament occlusion in C57Bl/6J mice. *Brain Res.* **997** (1), 15-23 (2004).

8 Au - Jiang, X. et al. Inducement and Evaluation of a Murine Model of Experimental Myopia. *Journal of Visualized Experiments.* doi:10.3791/58822 (143), e58822 (2019).

9 Miwa, Y. et al. Pharmacological HIF inhibition prevents retinal neovascularization with improved visual function in a murine oxygen-induced retinopathy model. *Neurochemistry International.* **128**, 21-31 (2019).

10 Adams, S., Pacharinsak, C. Mouse Anesthesia and Analgesia. *Current Protocols in Mouse Biology.* **5** (1), 51-63 (2015).

11 Au - Speetzen, L. J., Au - Endres, M., Au - Kunz, A. Bilateral Common Carotid Artery Occlusion as an Adequate Preconditioning Stimulus to Induce Early Ischemic Tolerance to Focal Cerebral Ischemia. *Journal of Visualized Experiments.* doi:10.3791/4387 (75), e4387 (2013).

12 Engel, O., Kolodziej, S., Dirnagl, U., Prinz, V. Modeling stroke in mice - middle cerebral artery occlusion with the filament model. *Journal of Visualized Experiments.* 10.3791/2423 (47), 2423 (2011).

13 Lee, D., Kang, H., Yoon, K. Y., Chang, Y. Y., Song, H. B. A mouse model of retinal hypoperfusion injury induced by unilateral common carotid artery occlusion. *Experimental Eye Research.* **201**, 108275 (2020).

14 Li, S. et al. Retro-orbital injection of FITC-dextran is an effective and economical method for observing mouse retinal vessels. *Molecular Vision.* **17**, 3566-3573 (2011).

15 Au - Tual-Chalot, S., Au - Allinson, K. R., Au - Fruttiger, M., Au - Arthur, H. M. Whole Mount Immunofluorescent Staining of the Neonatal Mouse Retina to Investigate Angiogenesis In vivo. *Journal of Visualized Experiments.* doi:10.3791/50546 (77), e50546 (2013).
16 Lee, D. et al. A Fairy Chemical Suppresses Retinal Angiogenesis as a HIF Inhibitor. *Biomolecules.* **10** (10) (2020).
17 Tomita, Y. et al. Pemafibrate Prevents Retinal Pathological Neovascularization by Increasing FGF21 Level in a Murine Oxygen-Induced Retinopathy Model. *International Journal of Molecular Sciences.* **20** (23), 5878 (2019).
18 Yamamoto, H., Schmidt-Kastner, R., Hamasaki, D. I., Yamamoto, H., Parel, J. M. Complex neurodegeneration in retina following moderate ischemia induced by bilateral common carotid artery occlusion in Wistar rats. *Experimental Eye Research.* **82** (5), 767-779 (2006).
19 Cheng, L., Yu, H., Yan, N., Lai, K., Xiang, M. Hypoxia-Inducible Factor-1α Target Genes Contribute to Retinal Neuroprotection. *Frontiers in Cellular Neuroscience.* **11**, 20-20 (2017).
20 Mole, D. R. et al. Genome-wide association of hypoxia-inducible factor (HIF)-1alpha and HIF-2alpha DNA binding with expression profiling of hypoxia-inducible transcripts. *The Journal of Biological Chemistry.* **284** (25), 16767-16775 (2009).
21 Majmundar, A. J., Wong, W. J., Simon, M. C. Hypoxia-Inducible Factors and the Response to Hypoxic Stress. *Molecular Cell.* **40** (2), 294-309 (2010).
22 Newman, E. A. Glial cell regulation of neuronal activity and blood flow in the retina by release of gliotransmitters. *Philosophical Transactions of the Royal Society B: Biological Sciences.* **370** (1672) (2015).
23 Vecino, E., Rodriguez, F. D., Ruzafa, N., Pereiro, X., Sharma, S. C. Glia–neuron interactions in the mammalian retina. *Progress in Retinal and Eye Research.* **51** , 1-40 (2016).
24 Symonds, C. The Circle of Willis. *British Medical Journal.* **1** (4906), 119 (1955).
25 Lo, W. B., Ellis, H. The circle before willis: a historical account of the intracranial anastomosis. *Neurosurgery.* **66** (1), 7-18; discussion 17-18 (2010).
26 Yang, G. et al. C57BL/6 strain is most susceptible to cerebral ischemia following bilateral common carotid occlusion among seven mouse strains: selective neuronal death in the murine transient forebrain ischemia. *Brain Research.* **752** (1), 209-218 (1997).
27 Farkas, E., Luiten, P. G. M., Bari, F. Permanent, bilateral common carotid artery occlusion in the rat: A model for chronic cerebral hypoperfusion-related neurodegenerative diseases. *Brain Research Reviews.* **54** (1), 162-180 (2007).
28 Morris, G. P. et al. A Comparative Study of Variables Influencing Ischemic Injury in the Longa and Koizumi Methods of Intraluminal Filament Middle Cerebral Artery Occlusion in Mice. *PLOS ONE.* **11** (2), e0148503 (2016).
29 Tsuchiya, D., Hong, S., Kayama, T., Panter, S. S., Weinstein, P. R. Effect of suture size and carotid clip application upon blood flow and infarct volume after permanent and temporary middle cerebral artery occlusion in mice. *Brain Research.* **970** (1-2), 131-139 (2003).
30 Kaelin, W. G., Ratcliffe, P. J. Oxygen Sensing by Metazoans: The Central Role of the HIF Hydroxylase Pathway. *Molecular Cell.* **30** (4), 393-402 (2008).
31 Pauly, M., Sruthi, R. Ptosis: evaluation and management. *Kerala Journal of Ophthalmolgy.* **31** (1), 11-16 (2019).
32 Averbuch-Heller, L., Leigh, R. J., Mermelstein, V., Zagalsky, L., Streifler, J. Y. Ptosis in patients with hemispheric strokes. *Neurology.* **58** (4), 620 (2002).

33 Dutton, J. *Atlas of clinical and surgical orbital anatomy, second edition*. Vol. 113 1364-1364 (2011).
34 Ritzel, R. M. et al. Early retinal inflammatory biomarkers in the middle cerebral artery occlusion model of ischemic stroke. *Molecular Vision.* **22** , 575-588 (2016).
35 Crespo-Garcia, S. et al. Individual and temporal variability of the retina after chronic bilateral common carotid artery occlusion (BCCAO). *PLOS ONE.* **13** (3), e0193961 (2018).
36 Qin, Y. et al. Functional and morphologic study of retinal hypoperfusion injury induced by bilateral common carotid artery occlusion in rats. *Scientific Reports.* **9** (1), 80 (2019).
37 Block, F., Grommes, C., Kosinski, C., Schmidt, W., Schwarz, M. Retinal ischemia induced by the intraluminal suture method in rats. *Neuroscience Letters.* **232** (1), 45-48 (1997).
38 Allen, R. S. et al. Progesterone Treatment in Two Rat Models of Ocular Ischemia. *Investigative Ophthalmology & Visual Science.* **56** (5), 2880-2891 (2015).
39 Miller, R. F., Dowling, J. E. Intracellular responses of the Müller (glial) cells of mudpuppy retina: their relation to b-wave of the electroretinogram. *Journal of Neurophysiology.* **33** (3), 323-341 (1970).
40 Block, F., Grommes, C., Kosinski, C., Schmidt, W., Schwarz, M. Retinal ischemia induced by the intraluminal suture method in rats. *Neuroscience Letters.* **232** (1), 45-48 (1997).
41 Lee, J.-H., Shin, J. M., Shin, Y.-J., Chun, M.-H., Oh, S.-J. Immunochemical changes of calbindin, calretinin and SMI32 in ischemic retinas induced by increase of intraocular pressure and by middle cerebral artery occlusion. *Anatomy & Cell Biology.* **44** (1), 25-34 (2011).
42 Li, S. Y. et al. Lycium barbarum polysaccharides reduce neuronal damage, blood-retinal barrier disruption and oxidative stress in retinal ischemia/reperfusion injury. *PLOS ONE.* **6** (1), e16380 (2011).
43 Furashova, O., Matthé, E. Retinal Changes in Different Grades of Retinal Artery Occlusion: An Optical Coherence Tomography Study. *Investigative Ophthalmology & Visual Science.* **58** (12), 5209-5216 (2017).
44 Zadeh, J. K. et al. Short-Time Ocular Ischemia Induces Vascular Endothelial Dysfunction and Ganglion Cell Loss in the Pig Retina. *International Journal of Molecular Sciences.* **20** (19) (2019).
45 Liu, S., Zhen, G., Meloni, B. P., Campbell, K., Winn, H. R. Rodent stroke model guidelines for preclinical stroke trials (1st edition). *Journal of Experimental Stroke & Translational Medicine.* **2** (2), 2-27 (2009).
46 Tang, Y. et al. Hypothermia-induced ischemic tolerance is associated with Drp1 inhibition in cerebral ischemia-reperfusion injury of mice. *Brain Research.* **1646**, 73-83 (2016).
47 Barone, F. C., Knudsen, D. J., Nelson, A. H., Feuerstein, G. Z., Willette, R. N. Mouse strain differences in susceptibility to cerebral ischemia are related to cerebral vascular anatomy. *Journal of Cerebral Blood Flow & Metabolism.* **13** (4), 683-692 (1993).
48 Pula, J. H., Yuen, C. A. Eyes and stroke: the visual aspects of cerebrovascular disease. *Stroke and Vascular Neurology.* **2** (4), 210 (2017).
49 Steele, E. C., Jr., Guo, Q., Namura, S. Filamentous middle cerebral artery occlusion causes ischemic damage to the retina in mice. *Stroke.* **39** (7), 2099-2104 (2008).
50 Sim, D. A. et al. The Effects of Macular Ischemia on Visual Acuity in Diabetic Retinopathy. *Investigative Ophthalmology & Visual Science.* **54** (3), 2353-2360 (2013).
51 Wu, K. K., Huan, Y. Streptozotocin-induced diabetic models in mice and rats. *Current*

Protocols in Pharmacology. **Chapter 5** , Unit 5.47 (2008).
52 Mubarak, A., Hodgson, J. M., Considine, M. J., Croft, K. D., Matthews, V. B. Supplementation of a high-fat diet with chlorogenic acid is associated with insulin resistance and hepatic lipid accumulation in mice. *Journal of Agricultural and Food Chemistry.* **61** (18), 4371-4378 (2013).
53 Ansari, S., Azari, H., McConnell, D. J., Afzal, A., Mocco, J. Intraluminal middle cerebral artery occlusion (MCAO) model for ischemic stroke with laser doppler flowmetry guidance in mice. *Journal of Visualized Experiments.* 10.3791/2879 (51), 2879 (2011).
54 Hedna, V. S. et al. Validity of Laser Doppler Flowmetry in Predicting Outcome in Murine Intraluminal Middle Cerebral Artery Occlusion Stroke. *Journal of Vascular and Interventional Neurology.* **8** (3), 74-82 (2015).

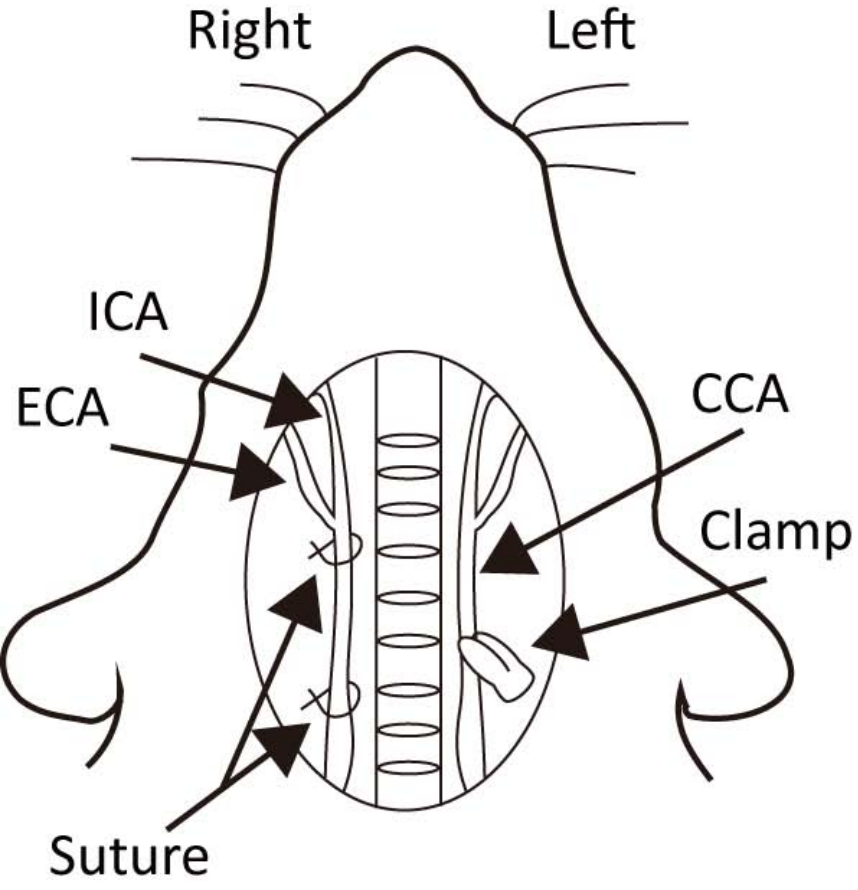

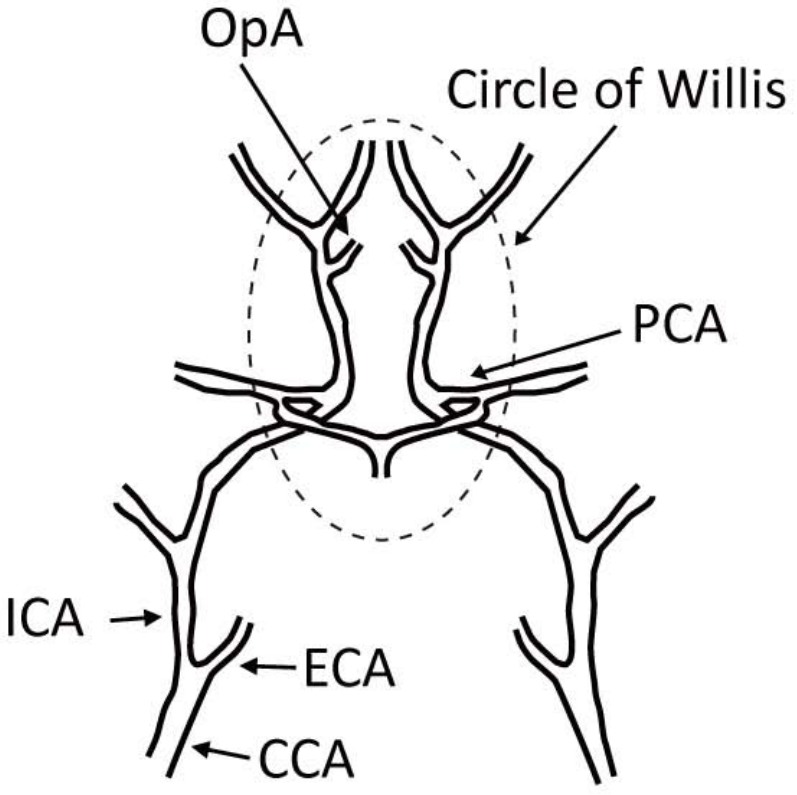

Reference images for scoring

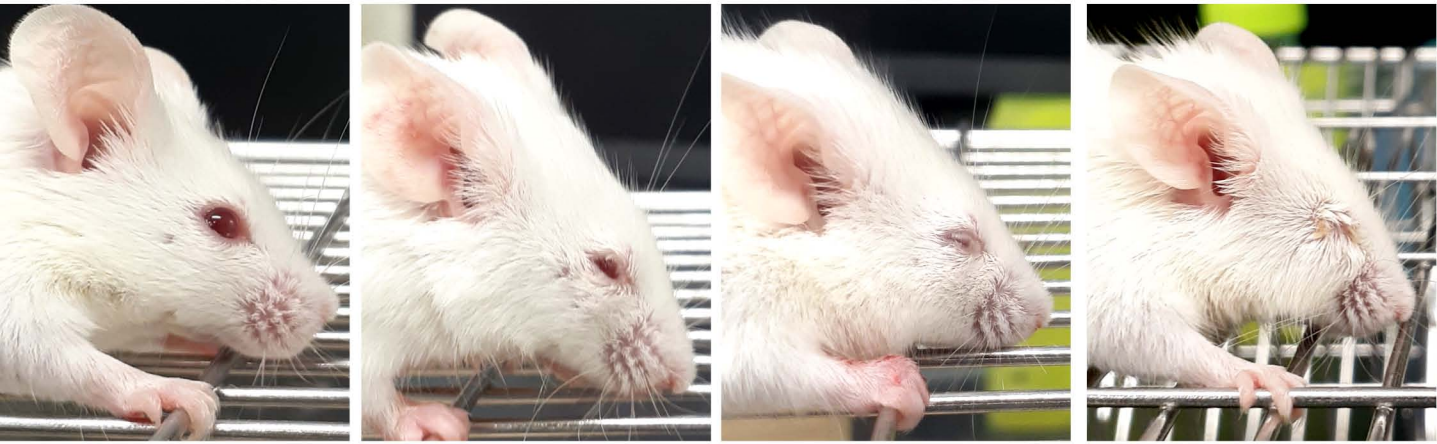

1 2 3 4

Low High

Severity

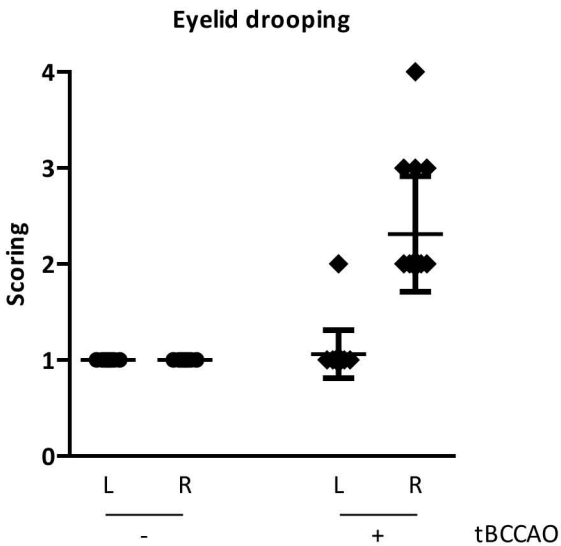

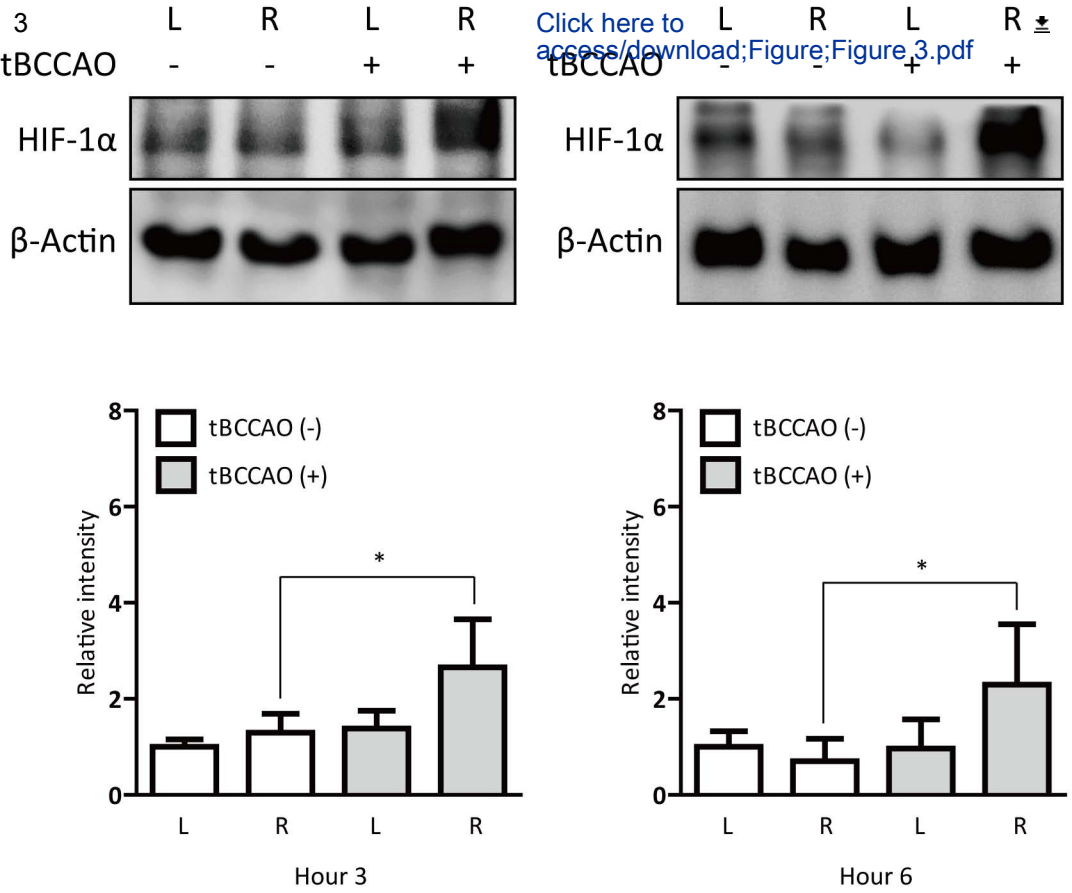
3
L
R
L
R
tBCCAO
-
-
+
+
HIF-1α
β-Actin
Click here to access/download;Figure;Figure 3.pdf
L
R
L
R
tBCCAO
-
-
+
+
HIF-1α
β-Actin
tBCCAO (-)
tBCCAO (+)
Relative intensity
8
6
4
2
0
*
L
R
L
R
Hour 3
tBCCAO (-)
tBCCAO (+)
Relative intensity
8
6
4
2
0
*
L
R
L
R
Hour 6

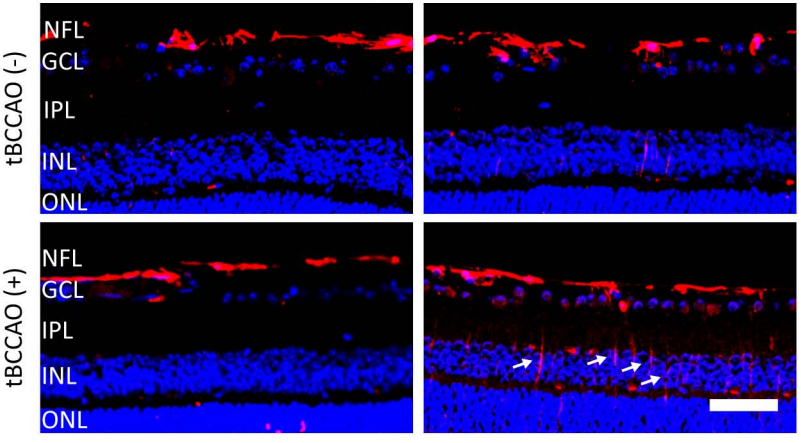

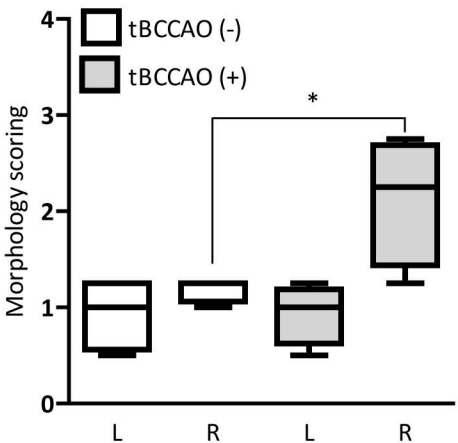

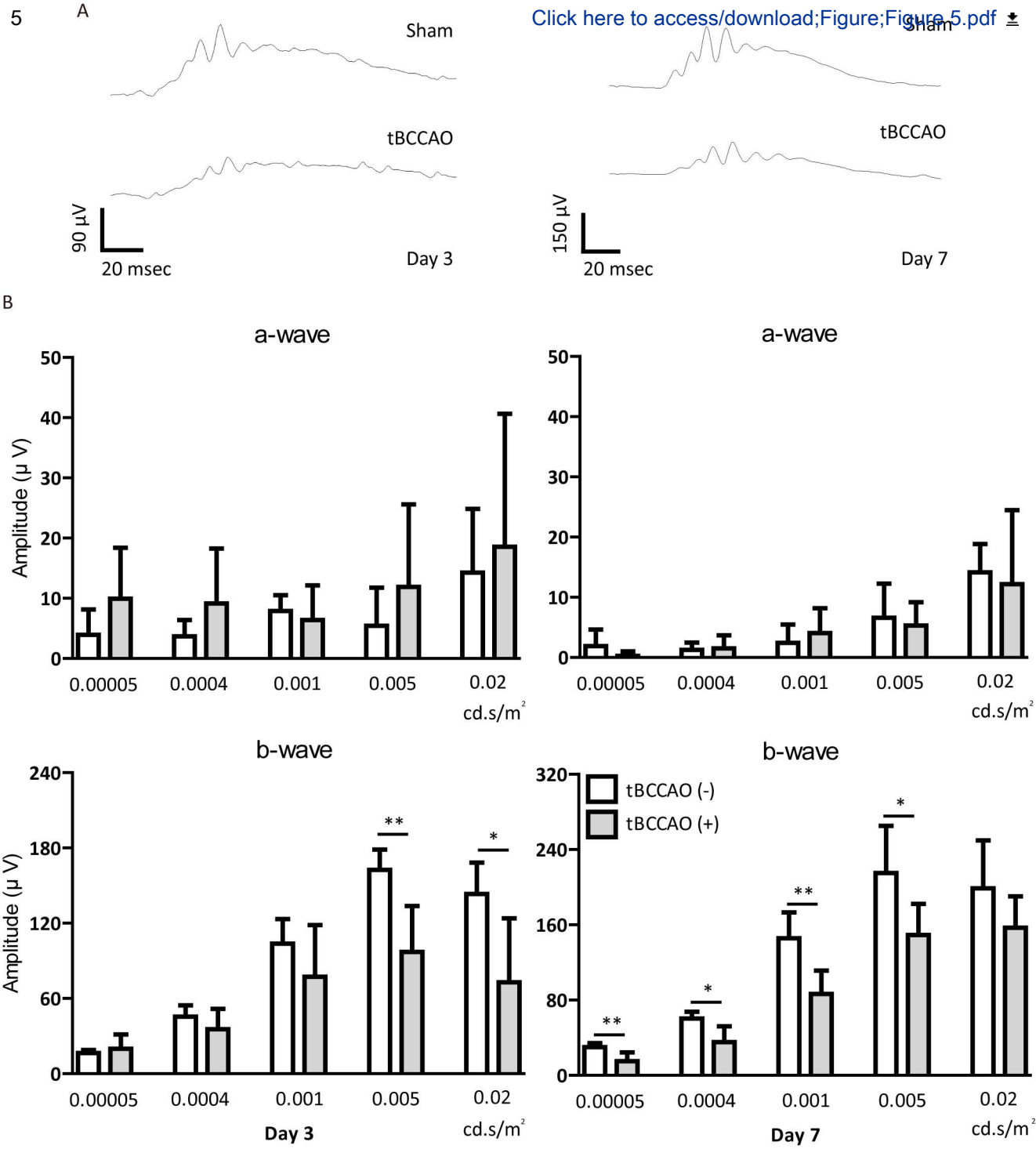

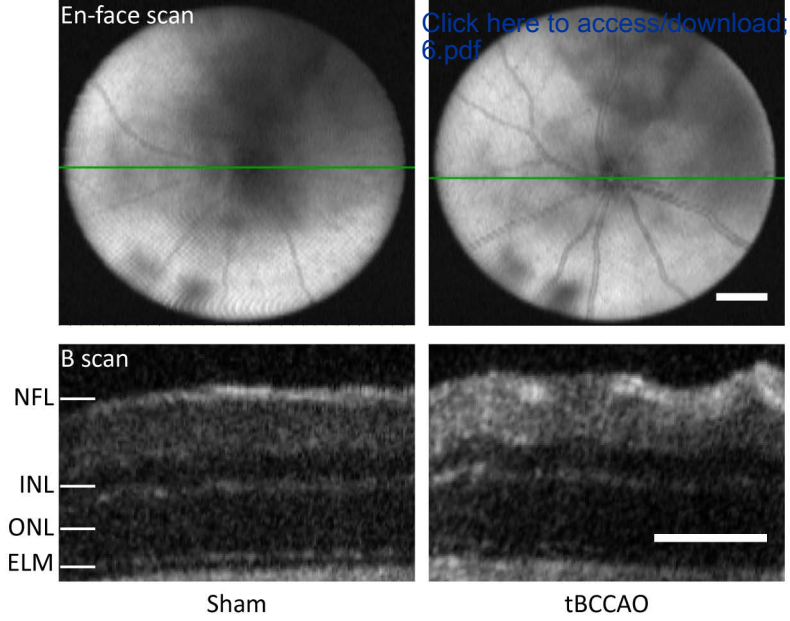

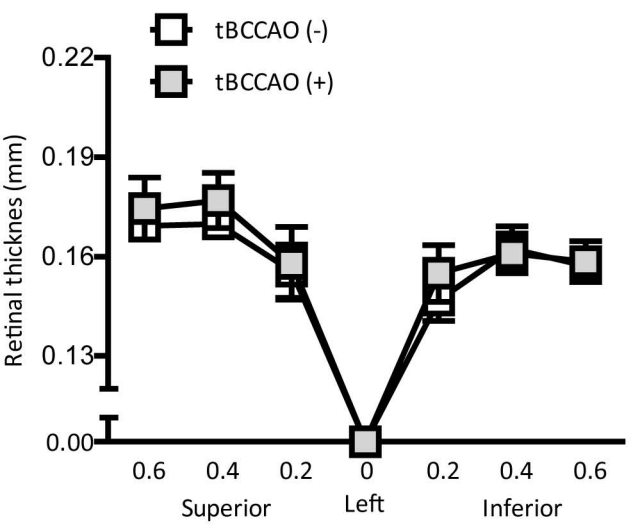

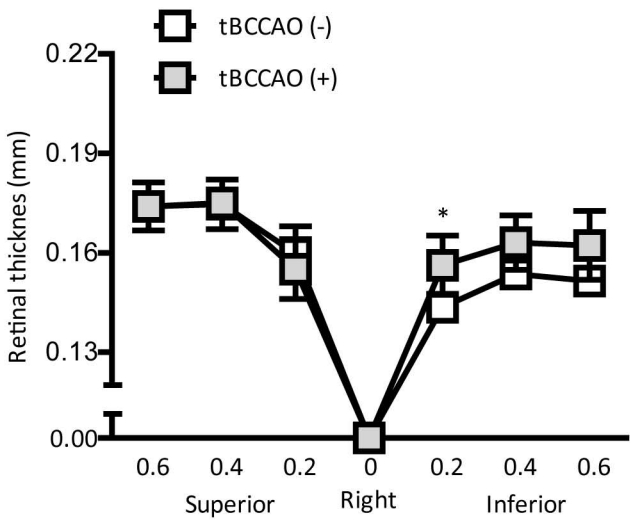

Table 1. Primer list

Name	Direction	Sequence (5' → 3')	Accession number
Hprt	Forward	TCAGTCAACGGGGGACATAAA	NM_013556.2
	Reverse	GGGGCTGTACTGCTTAACCAG	
Vegf	Forward	CCTGGTGGACATCTTCCAGGAGTACC	AY707864.1
	Reverse	GAAGCTCATCTCTCCTATGTGCTGGC	
Bnip3	Forward	GCTCCCAGACACCACAAGAT	NM_009760.4
	Reverse	TGAGAGTAGCTGTGCGCTTC	
Epo	Forward	GGCCATAGAAGTTTGGCAAG	NM_007942
	Reverse	CCTCTCCCGTGTACAGCTTC	

Name of Material/ Equipment	Company	Catalog Number	Comments/Description
Atipamezole hydrochloride	Zenoaq	Antisedan	For anti-anesthesia
Applied Biosystems 7500 Fast	Applied Biosystems	-	For qPCR
Butorphanol tartrate	Meiji Seika Pharma	Vetorphale	For anesthesia
BZ-II Analyzer	KEYENCE	-	For an image merge
BALB/cAJc1	CLEA	-	Mouse strain
β-Actin (8H10D10) Mouse mAb	CST	3700	For western blot
Clamp Forcep	World Precision Instruments	WPI 500451	For surgery
Dumont forceps #5	Fine Science Tools	11251-10	For surgery
DAPI solution	Dojindo	340-07971	For IHC
Envisu SD-OCT system	Leica	R4310	For OCT
FITC-dextran	Merk	FD2000S	For retinal blood perfusion
Fluorescence microscope	KEYENCE	BZ-9000	For fluorescence detection
Gatifloxacin hydrate	Senju Pharmaceutical	Gachifuro	For anti-bacterial infection
GFAP Monoclonal Antibody (2.2B10)	Thermo	13-0300	For IHC
Heating pad	Marukan	RH-200	For surgery
HIF-1α (D1S7W) XP Rabbit mAb	CST	36169	For western blot
ImageQuant LAS 4000 mini	GE Healthcare	-	For chemiluminescence
Midazolam	Sandoz K.K	SANDOZ	For anesthesia
Microtome Tissue-Tek TEC 6	Sakura	-	For sectioning
Medetomidine	Orion Corporation	Domitor	For anesthesia
Needle holder	Handaya	HS-2307	For surgery
PuREC	MAYO Corporation	-	For ERG
Scissor	Fine Science Tools	91460-11	For surgery
Sodium hyaluronate	Santen Pharmaceutical	Hyalein	For eye lubrication
Tropicamide/Penylephrine hydrochloride	Santen Pharmaceutical	Mydrin-P	For mydriasis
6-0 silk suture	Natsume	E12-60N2	For surgery

Oct 27, 2020

Kyle Jewhurst, PhD

Science Editor, *JoVE*

Dear Dr. Jewhurst,

We appreciate your careful review of our manuscript entitled ‘A murine model of ischemic retinal injury induced by transient bilateral common carotid artery occlusion’. As followed your suggestion, we added comments on our manuscript. After this revision, we are confident that the article has been much improved. For emphasis, new text added to the manuscript is colored red, and the reviewers’ original questions are italicized and colored blue in this document. We believe that the revision addresses all the comments raised by you and the reviewers and hope that it will be published in *JoVE*.

Sincerely yours,

Corresponding authors

Toshihide Kurihara, MD, PhD

Laboratory of Photobiology, Department of Ophthalmology, Keio University School of Medicine; 35 Shinanomachi, Shinjuku-ku, Tokyo 160-8582, Japan.

Tel: +81-3-5363-3204, Fax: +81-3- 5363-3274

E-mail: kurihara@z8.keio.jp

Kazuo Tsubota, MD, PhD

Professor and Department Chair, Department of Ophthalmology, Keio University School of Medicine; 35 Shinanomachi, Shinjuku-ku, Tokyo 160-8582, Japan.

Tel: +81-3-5363-3269, Fax: +81-3- 3358-5961

E-mail: tsubota@z3.keio.jp

1. *Please revise the following lines to avoid previously published text: 40-42, 43-45, 59-62, 443-446, 465-466.*

Response 1: Thank you for your corrections. We revised the manuscript as requested.

[Line 40-42 and 43-45]

Diverse vascular diseases such as diabetic retinopathy, occlusion of retinal veins or arteries and ocular ischemic syndrome can lead to retinal ischemia. To investigate pathological mechanisms of retinal ischemia, relevant experimental models need to be developed. Anatomically, a main retinal blood supplying vessel is the ophthalmic artery (OpA) and OpA originates from the internal carotid artery of the common carotid artery (CCA). Thus, disruption of CCA could effectively cause retinal ischemia.

[Line 59-62]

The retina is susceptible to vascular diseases as oxygen is delivered through blood vessels. Various types of vascular diseases, such as diabetic retinopathy and retinal blood vessel (veins or arteries) occlusion, can induce retinal ischemia. To investigate pathological mechanisms of retinal ischemia, reproducible and clinically relevant experimental models of retinal ischemia are considered necessary. Middle cerebral artery occlusion (MCAO) by insertion of an intraluminal filament is the most generally utilized method for the development of in vivo rodent models of experimental cerebral ischemia2,3.

[Line 443-446 and 465-466]

The phenotype of a droopy eyelid has been suggested as a presenting sign or a pathophysiological symptom of severe neurological conditions, especially ischemic stroke31,32. The muscle associated with a droopy eyelid is levator palpebrae superioris33. This muscle is supplied by the lateral palpebral artery which is one of branches derived from OpA. Hence, when OpA, which supplies the retina, is affected, eyelid drooping could be seen.

For consistent outcomes, anesthetic time and length of surgical procedures as well as other factors such as weights and ages of experimental models and their body temperatures during and after the surgery should be standardized.

2. *Please highlight up to 3 pages of protocol text for inclusion in the protocol section of the video. This is a hard production limit to ensure that videography can occur in a single day. Please highlight the key parts of the experiments and enough details to tell a cohesive story.*

Response 1: Thank you for your instruction. We highlighted the key parts as requested.

[Line 82-152]

1. Preparation of surgical instruments and animals

1.1. Autoclave surgical instruments and keep them in 70% ethyl alcohol. Prior to each new surgical procedure, clean surgical instruments carefully using 70% ethyl alcohol.

1.2. Prepare male BALB/cAJc1 mice (6 weeks old, 26-28 kg) in a specific-pathogen-free (SPF) room to maintain sterile conditions before, during and after the surgery.

2. Transient bilateral common carotid artery occlusion (tBCCAO)

2.1. Put a mouse under anesthesia via intraperitoneal injection with a combination of midazolam (40 μg/100 μL), medetomidine (7.5 μg/100 μL) and butorphanol tartrate (50 μg/100 μL), termed “MMB”, as previously described8,9. Hold the mouse’s back skins to keep the mouse away from bumping its eyes until the mouse is completely anesthetized.

2.1.1. Judge the depth of anesthesia by pinching the mouse toe until it has no response, of which method is commonly used for checking complete anesthesia10.

NOTE: Generally, less than 5 min are required for mice to fall asleep. Proper recipes for general anesthesia may be different by institutions.

2.2. Apply one drop of 0.1% purified sodium hyaluronate eye drop solution to the eyes to prevent dryness on the eyes under anesthesia.

2.3. Place the mouse on its back and fix the mouse's paws using adhesive tapes.

2.4. Disinfect the neck area of the mouse using 70% ethyl alcohol before the surgery.

NOTE: Additional clipping of the fur was not performed as this may cause subsequent skin inflammation11,12.

2.5. Perform sagittal incision of the neck by a scissor (Figure 1).

NOTE: Incision needs to be made on the midline between the neck, sternum and trachea.

2.6. Separate both salivary glands carefully using two forceps and mobilize them to visualize the underlying CCAs.

2.7. Isolate the right CCA carefully from the respective vagal nerves and accompanying veins without harming their structures, and place two 6-0 silk sutures under the CCA. Tie the two ties tightly to block the blood flow (Figure 1).

NOTE: During the procedure, small veins could be damaged. If bleeding is seen, wiping is required to visualize the CCAs clearly.

2.8. Find the left CCA carefully from the respective vagal nerves and accompanying veins without harming their structures, and occlude the left CCA for 2 seconds by a clamp (Figure 1).

NOTE: A 6-0 silk suture needle is needed to be placed under the left CCA to mark a site for clamping.

2.9. After reopening of the left CCA, suture wounds of the neck by a 6-0 silk suture and apply a dab of antibiotic (50 µL) onto the neck to inhibit bacterial infection.

NOTE: Softly remove a clamp to avoid damaging the arterial wall when reopening of the left CCA.

2.10. Inject 0.75 mg/kg of atipamezole hydrochloride intraperitoneally to the mice to help

the mouse recovered from deep anesthesia quickly. Return the mouse to a mouse cage with pre-heated pads.

NOTE: Do not let the mouse left unattended until the mouse regains sufficient consciousness to maintain sternal recumbency.

2.11. Inject 0.4 mg/kg of butorphanol tartrate to the mouse for the management of pain when the mouse wakes up.

NOTE: The protocol can be paused here. As a first hint for successful tBCCAO, eyelid drooping of the mouse can be observed (Figure 2).

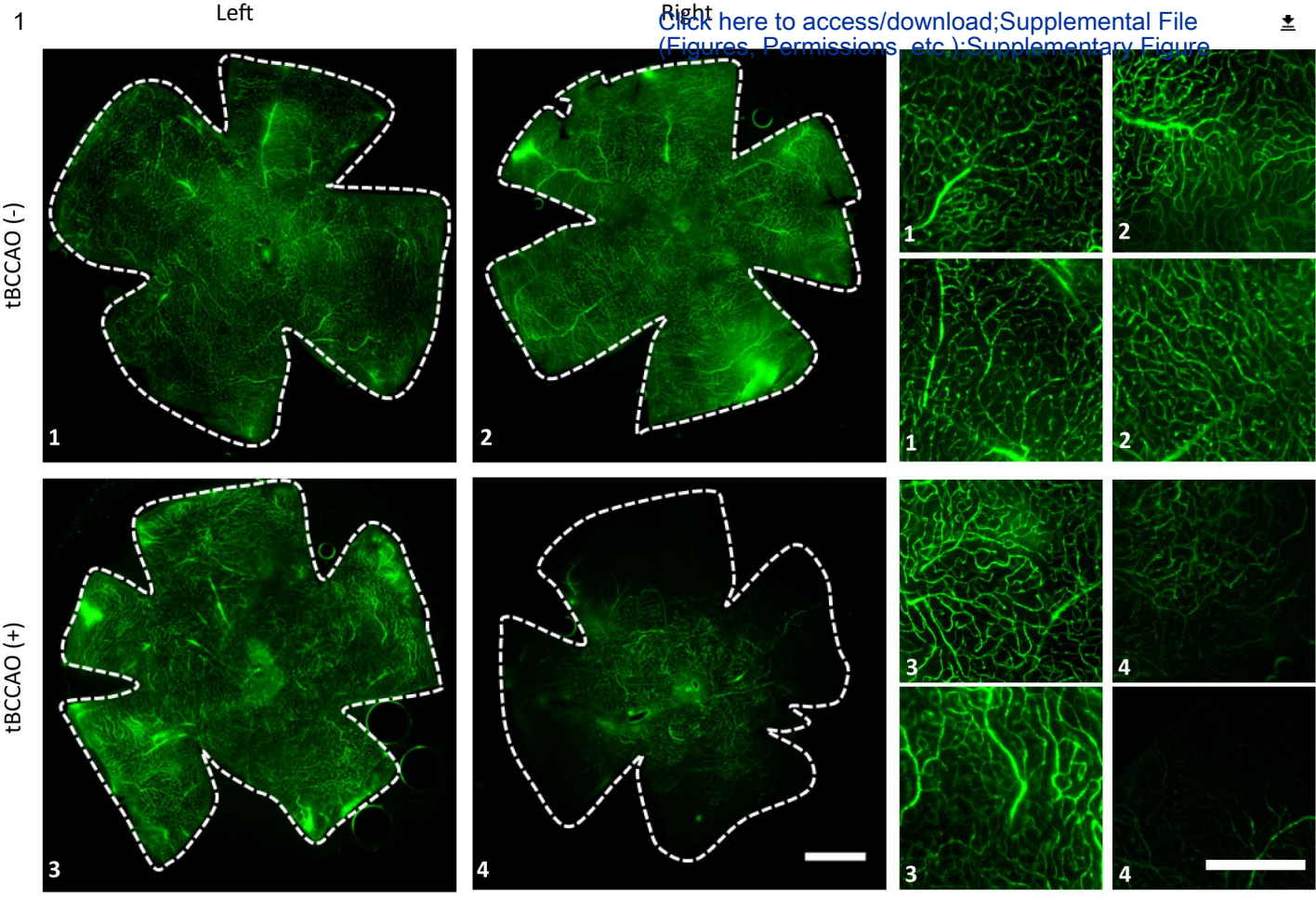

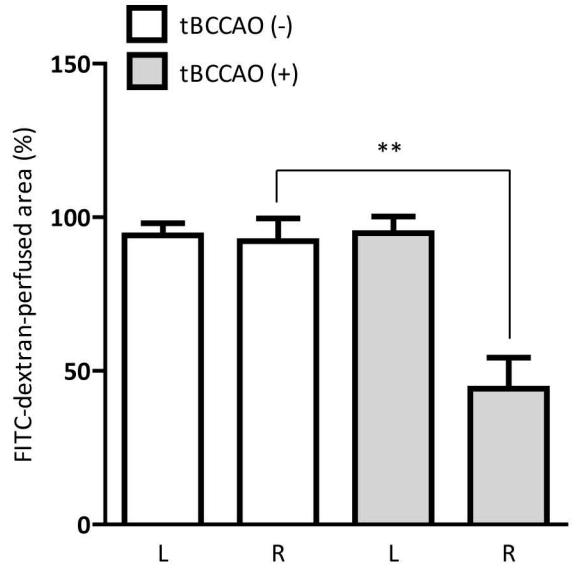

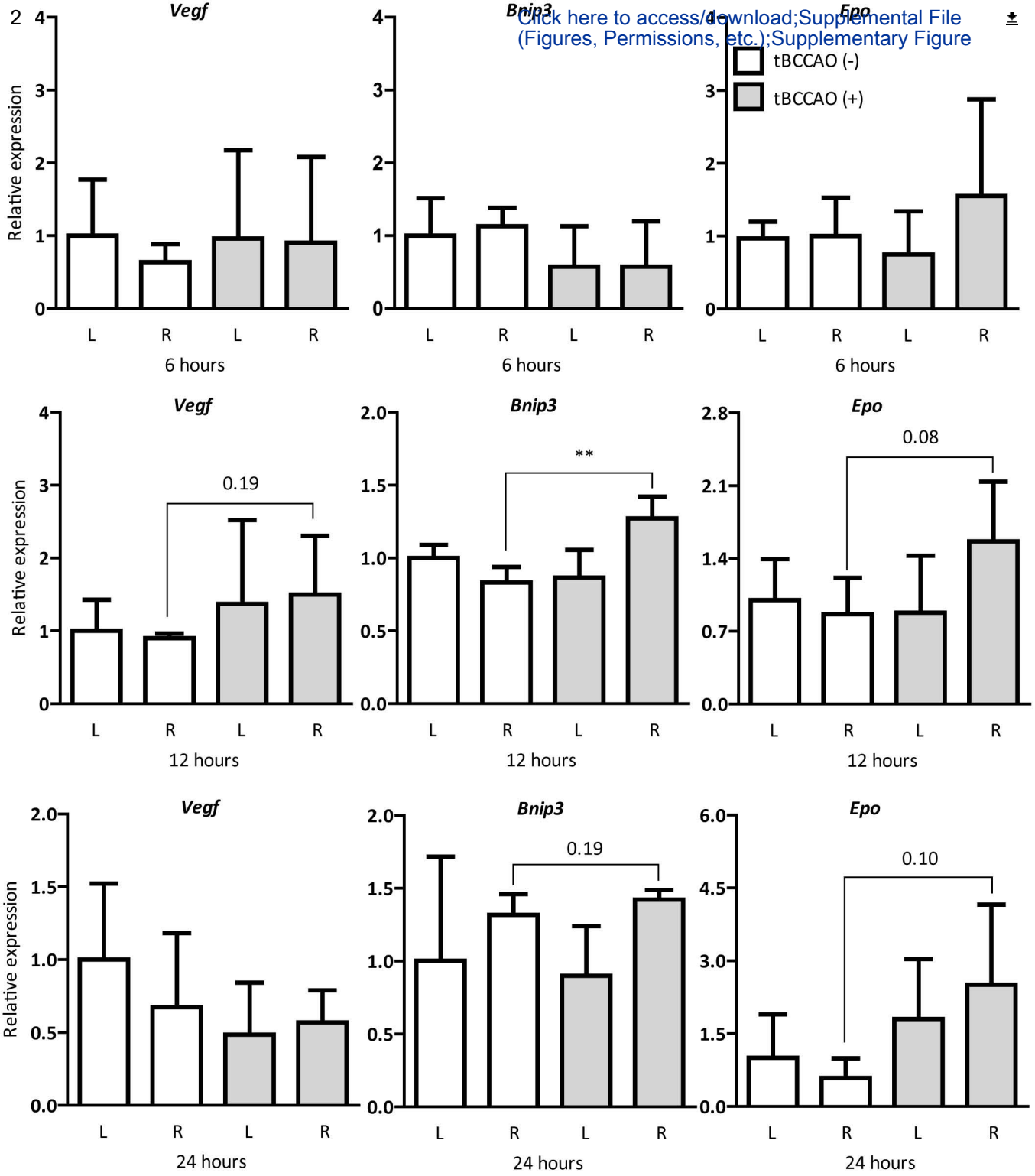

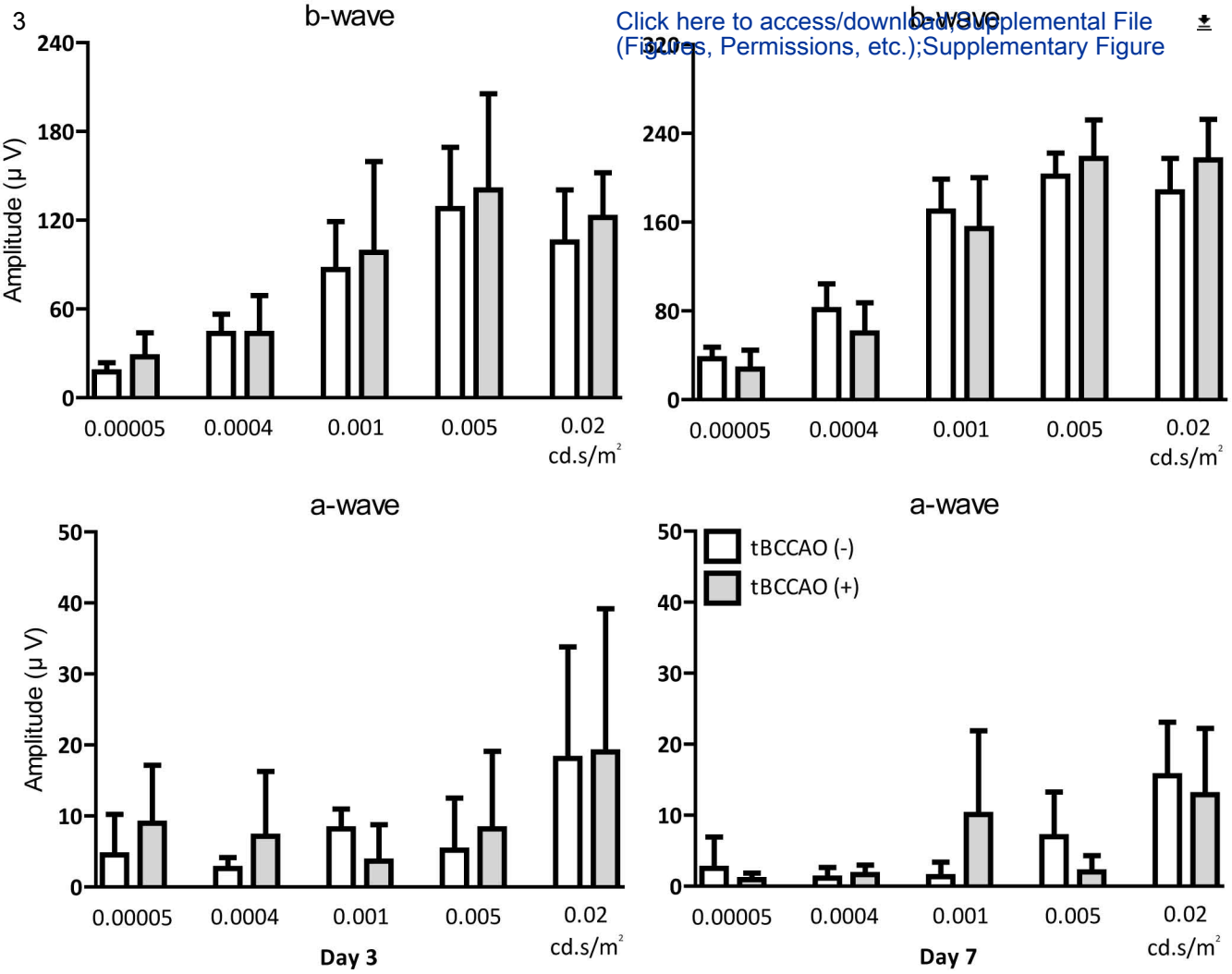

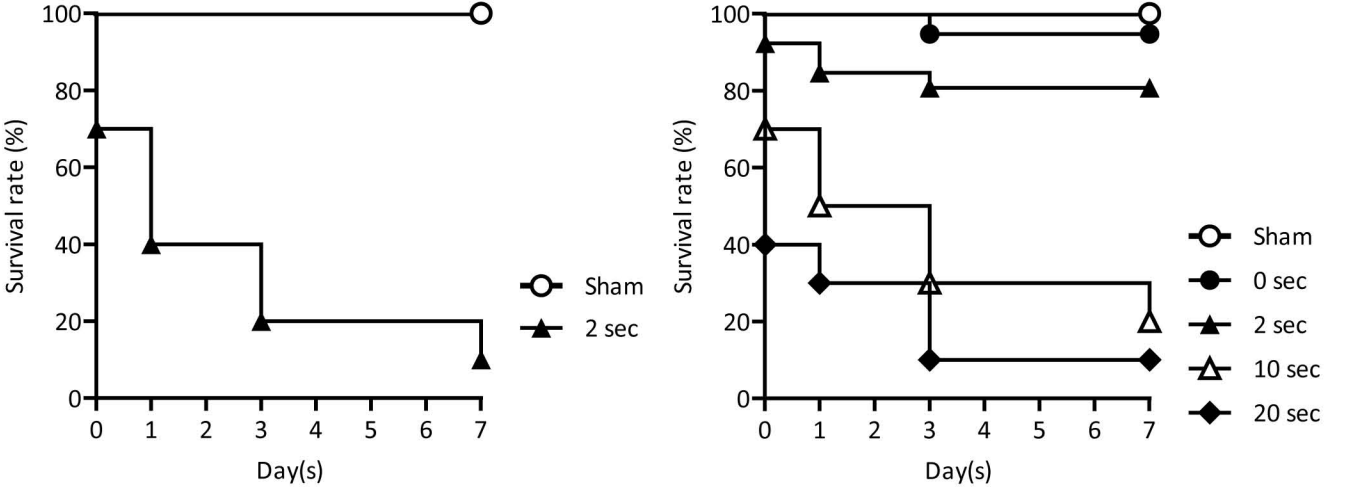

5